JOURNAL OF MATERIALS SCIENCE **34** (1999) 2703–2713

Sensing damage in carbon fiber and its polymer-matrix and carbon-matrix composites by electrical resistance measurement

XIAOJUN WANG, SHOUKAI WANG, D.D.L.CHUNG
Composite Materials Research Laboratory, State University of New York at Buffalo, Buffalo, NY 14260-4400

Fatigue damage was sensed in real time in continuous carbon fiber and its polymer-matrix and carbon-matrix composites by electrical resistance measurement in the fiber direction. In a polymer-matrix composite, fiber breakage overshadows fiber damage in causing the resistivity of the composite to increase irreversibly. In a carbon-matrix composite, fiber breakage and matrix cracking caused the resistivity to increase irreversibly, such that these two mechanisms cannot be distinguished. Fatigue damage was detected from 50% of the fatigue life onward for the polymer-matrix composite, and from 0% of the fatigue life onward for the carbon-matrix composite.

1. Introduction

Damage occurs during use of a structure, whether the structure is a civil structure, an aerospace structure or machinery. If a structure encounters dynamic loading during use, as in the case of a helicopter rotor or a turbine blade, fatigue is a common cause of damage. For the purpose of hazard mitigation and usage maximization, it is important to sense the damage of a structure, whether during use (in real time) or between uses. Real time sensing is safer than sensing between uses, but it is technically more difficult. Instead of sensing, a more traditional method involves the use of past experience on similar structures to predict the service life of a particular structure. This method tends to be not reliable, because similar structures are bound to be different, especially if they are fabricated from composite materials, which tend to have flaws (e.g., fiber residual stress, fiber waviness, delamination, etc.) built in during composite material fabrication. The sensing of damage is conventionally performed by the use of attached or embedded damage sensors, such as optical fibers, acoustic sensors, etc. However, these sensors add to the cost and are limited in durability. In addition, the sensing volume and spatial resolution are limited. In the case of embedded sensors, the presence of the sensors degrades the mechanical properties of the structure.

Composite materials involving fiber reinforcements have become common structural materials. Among the various types of fibers, carbon fibers have become quite dominant due to their high strength, high modulus, low density and temperature resistance. Carbon fibers are used to reinforce polymers, carbon, cement and metals. If the carbon fiber composite itself provides damage sensing, then the conventional attached or embedded sensors are not necessary. This would mean reduced cost, greater durability, larger sensing volume and absence of mechanical property degradation (due to embedded sensors). Therefore, this paper addresses damage sensing using carbon fiber composites, i.e., the structural materials themselves.

Carbon fibers are electrically conductive. This behavior causes an increase in electrical resistance in response to damage, thus enabling damage sensing. In a composite with continuous carbon fibers as the reinforcement, fiber breakage causes the resistivity of the composite in the fiber direction to increase, thus enabling damage sensing in the composite [1–11]. In case the matrix of the composite is carbon, which is electrically conducting, matrix cracking causes the resistivity of the composite to increase, thus also enabling damage sensing. This paper provides a systematic study of damage sensing in (i) a single carbon fiber, (ii) a polymer-matrix composite with continuous carbon fibers, and (iii) a carbon-matrix composite with continuous carbon fibers. Carbon fiber polymer-matrix composites are used for aerospace, automobile and marine structures, sporting goods and turbine blades. Carbon fiber carbon-matrix composites (also called carbon-carbon composites) are used for high temperature aerospace structures, as the carbon matrix makes them much more temperature resistant than a polymer matrix. In addition, carbon-carbon composites are used for biomedical implants, due to the biocompatibility of carbon. Damage sensing is to be distinguished from strain sensing [12]; damage is irreversible but strain can be reversible.

2. A single carbon fiber

Previous electromechanical study of carbon fibers reported that, for low-modulus carbon fibers, the electrical resistance increases reversibly with tensile strain and decreases reversibly with compressive strain, mainly due to dimensional change rather than resistivity change [13–17]. However, damage, which would have

caused an irreversible resistivity change, was not addressed. The objective of this section is to investigate the effect of damage on the resistivity of the carbon fiber.

The carbon fiber used was 10E-Torayca T-300 (unsized, PAN-based), of diameter 7 μm, density 1.76 g/cm^3, tensile modulus 221 ± 4 GPa, tensile strength 3.1 ± 0.2 GPa and ultimate elongation 1.4%. The electrical resistivity was $(2.2 \pm 0.5) \times 10^{-3}\ \Omega \cdot$ cm, as measured by using the four-probe method and silver paint electrical contacts on single fibers. Single fiber electromechanical testing was conducted by measuring the electrical resistance during static and cyclic tension. The DC resistance was measured by using the four-probe method, using silver paint for the electrical contacts. The outer two contacts (50 mm apart) were for passing a current; the inner two contacts (40 mm apart, also taken as the gage length for strain measurement) were for voltage measurement (Fig. 1). A Keithley 2001 multimeter was used. Away from the four contacts, the single fiber was attached vertically with adhesive (60 mm apart) to a piece of paper with a rectangular hole (with rounded corners) cut in it (Fig. 1). Prior to vertical tension application, the paper was cut horizontally along the dashed lines shown in Fig. 1. The tension was under load control, as provided by a screw-type mechanical testing system (Sintech 2/D). The crosshead speed was 0.1 mm/min. The strain was obtained from the crosshead displacement.

Fig. 2 shows typical plots of the fractional increase in resistance ($\Delta R/R_0$), stress and strain simultaneously obtained during static tensile testing up to failure. $\Delta R/R_0$ increased monotonically with strain/stress, with a slight negative deviation from linearity. The extent of negative deviation varied from sample to sample. About 10% of the samples were anomalous in that $\Delta R/R_0$ decreased a little bit before increasing monotonically. This anomaly was also reported in [1] Table I shows the analysis of the results in Fig. 2a. The gage factor (or strain sensitivity), given by the measured $\Delta R/R_0$

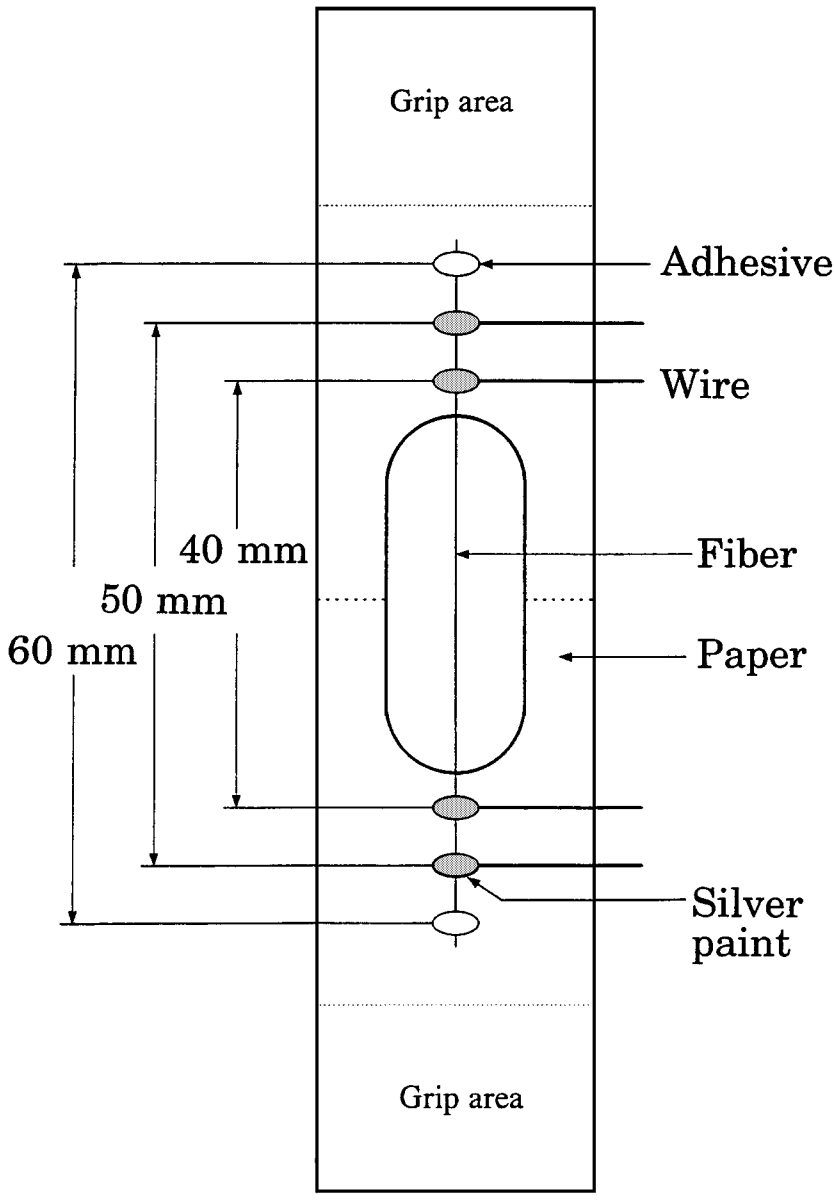

Figure 1 Configuration for bare single fiber electromechanical testing. The single fiber (solid vertical line) is adhered to a sheet of paper using adhesive (open ellipses). Four silver paint electrical contacts (dotted ellipses) are made to the fiber. The sheet of paper has a rectangular (with rounded corners) hole cut in its middle. The paper is cut along the horizontal dashed line at its middle prior to testing.

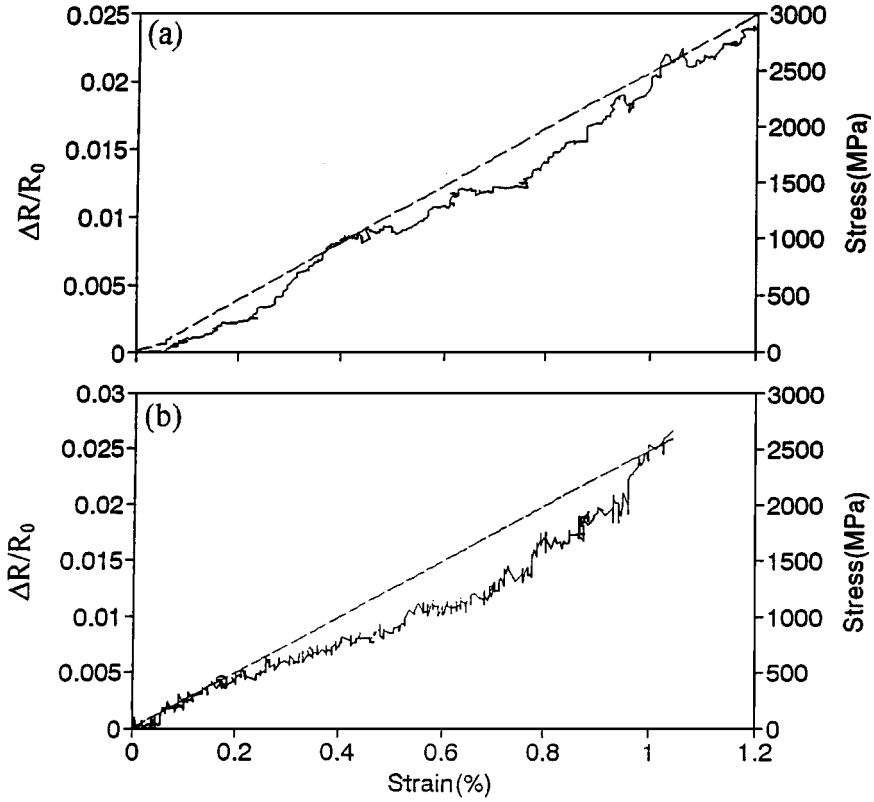

Figure 2 $\Delta R/R_0$ (solid curve), stress (dashed curve) and strain simultaneously obtained during static tension up to failure of a bare single fiber.

TABLE I Electromechanical behavior of single bare carbon fiber under static tension (data correspond to Fig. 2a)

	$\Delta R/R_0\,(10^{-3})$		Gage factor[b]	
Strain (%)	Measured	Calculated [a]	Measured	Calculated
0.40	7.4	6.2	1.9	1.5
0.50	8.8	7.7	1.8	1.5
0.60	11	9.2	1.8	1.6
0.70	13	10	1.9	1.6
0.80	14	12	1.8	1.6
0.90	16	14	1.8	1.6
1.0	19	16	1.9	1.6
1.1	21	17	1.9	1.6

[a]Calculated from change in dimensions.

$$\frac{\Delta R}{R_0} = \frac{1+\varepsilon}{1-2\nu\varepsilon} - 1,$$

where ε = strain and ν = Poisson ratio = 0.27.
[b]$\Delta R/R_0$ divided by the strain.

divided by the strain, was 1.8–1.9 throughout the whole range of strain. The $\Delta R/R_0$ calculated from the change in dimensions was less than but quite close to the measured $\Delta R/R_0$ at every strain value.

Fig. 3 shows plots of $\Delta R/R_0$ vs. time and strain vs. time, simultaneously obtained during the first 2 cycles of tensile loading at stress amplitudes equal to 18, 58 and 83% of the fracture stress respectively. Table II shows the analysis of such results for five values of the stress amplitude. The strain and $\Delta R/R_0$ were totally reversible at low values of the stress amplitude (up to 58% of the fracture stress), but their irreversible components increased with stress amplitude at high values of the stress amplitude. At the highest stress amplitude of 83% of the fracture stress, the extent of irreversibility of strain and $\Delta R/R_0$ increased slightly with cycle number (Fig. 3c and Table II). At the intermediate stress amplitude of 58.1% of the fracture stress, the strain was totally reversible but $\Delta R/R_0$ was not (Fig. 3b). A nonzero irreversible portion of $\Delta R/R_0$ was associated with a nonzero fractional decrease in the elastic modulus from the first cycle to the second cycle. The greater was the irreversible portion of $\Delta R/R_0$, the greater was the fractional decrease in modulus. The gage factor, given by the reversible portion of $\Delta R/R_0$ divided by the reversible strain, was 1.9–2.3 at all stress amplitudes for both Cycles 1 and 2. The $\Delta R/R_0$ calculated from the change in dimensions was less than the measured reversible $\Delta R/R_0$ at every stress amplitude.

Comparison of the calculated and measured reversible $\Delta R/R_0$ shows that dimensional change is the main cause of the observed reversible resistance change. However, dimensional change does not account for all of the observed reversible resistance change. A reversible structural change that gives rise to a resistivity change may contribute to the cause. A structural change upon tension of heat-treated benzene-derived graphite fibers had been suggested by Raman scattering [16].

The observed irreversible resistance change is attributed to damage, as supported by the accompanying decrease in the elastic modulus. Damage occurs at stress amplitudes $\geq$58% of the fracture stress and increases with increasing stress amplitude. Irreversible strain occurs at stress amplitudes $\geq$73% of the fracture stress and increases with increasing stress amplitude. Thus, damage occurs not only when there is irreversible strain, but also at a stress amplitude of 58% of the fracture stress,

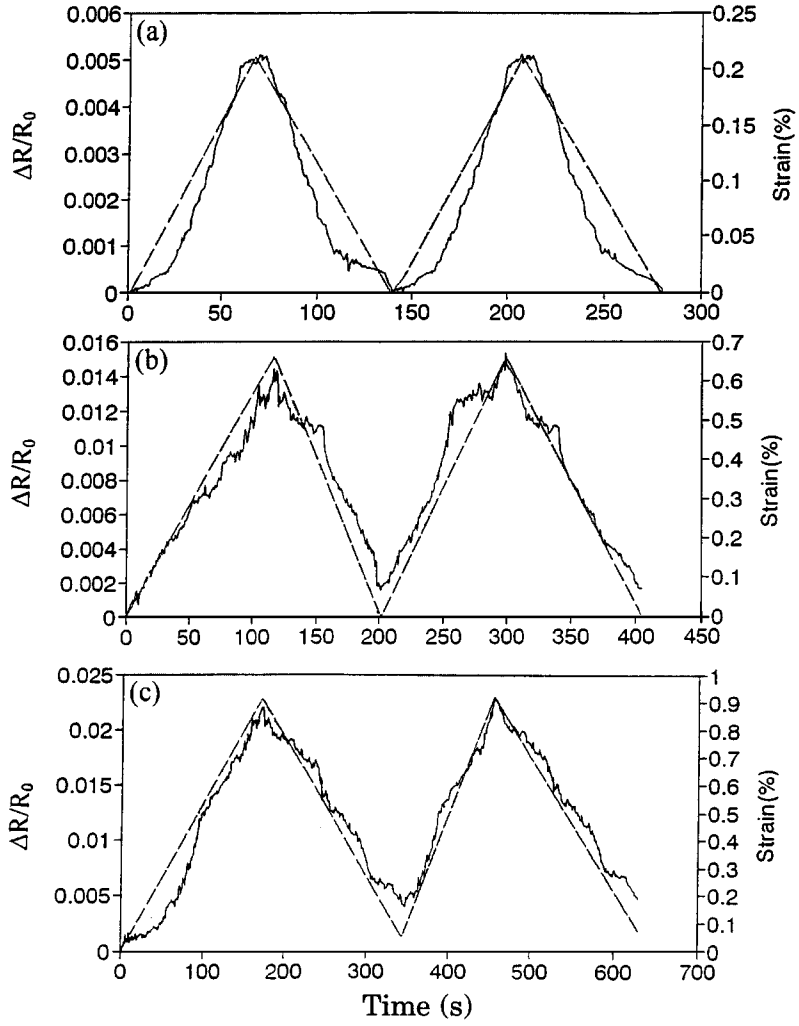

Figure 3 Plots of $\Delta R/R_0$ vs. time (solid curve) and of strain vs. time (dashed curve) during two cycles of cyclic tension of a bare single fiber at a maximum stress of (a) 19% of the fracture stress, (b) 58% of the fracture stress and (c) 83% of the fracture stress.

at which the strain is totally reversible. This suggests that damage can occur even in the regime of elastic deformation.

The gage factor values given in Table I are slightly lower than those of Table II because the total strain was considered in Table I and the reversible strain was considered in Table II. Nevertheless, in both cases, the gage factor is quite independent of strain/stress for essentially the whole range of strain/stress up to fracture. The gage factor values are higher than the values in the range 1.3–1.7 reported in [1] (probably due to the difference in carbon fiber), but are close to those in the range 1.95–2.02 reported in [14].

Even at a stress amplitude of 83% of the fracture stress, the irreversible portion of $\Delta R/R_0$ is much smaller than the reversible portion. Nevertheless, the irreversible portion can be useful as an indicator of the amount of damage, so that the carbon fiber becomes a sensor of its own damage. This damage should be distinguished from fiber breakage, which would cause the irreversible $\Delta R/R_0$ to be ∞.

In summary, this section shows that (i) the electromechanical behavior of carbon fiber is not totally reversible when the tensile stress is $\geq$58% of the fracture stress, though the irreversible resistance change is small compared to the reversible resistance change, (ii) the reversible resistance change is mainly due to the dimensional change associated with elastic deformation, though the dimensional change cannot explain the entire reversible resistance change, (iii) the irreversible resistance change is associated with an irreversible decrease in the tensile modulus and, in most cases, is also associated with an irreversible strain, (iv) the irreversible resistance change increases with tensile stress and increases slightly with tensile cycle number (from 1 to 2), (v) the irreversible resistance increase is attributed to fiber damage, and (vi) the gage factor (reversible $\Delta R/R_0$ per unit reversible strain) is 1.9–2.3 and is quite independent of stress or cycle number (from 1 to 2).

3. A polymer-matrix composite with continuous carbon fibers

Section 2 describes the behavior of a single carbon fiber. This section extends the work to a polymer-matrix composite containing a large number of continuous unidirectional carbon fibers that are of the same type as in Section 2 for a single fiber.

Composite samples were constructed from individual layers cut from a 12 in. (30 cm) wide unidirectional carbon fiber prepreg tape manufactured by ICI

TABLE II Electromechanical behavior of single bare carbon fiber under cyclic tension

Maximum stress / Fracture stress	18.8%[c]	38.5%[c]	58.1%[d]	73.1%[d]	83.0%[e]
Strain (%)					
Reversible					
Cycle 1	0.22 ± 0.02	0.41 ± 0.05	0.65 ± 0.08	0.73 ± 0.10	0.86 ± 0.10
Cycle 2	0.22 ± 0.02	0.41 ± 0.06	0.65 ± 0.10	0.72 ± 0.13	0.85 ± 0.12
Irreversible					
Cycle 1	$0.00 + 0.00$	$0.00 + 0.00$	$0.00 + 0.00$	0.04 ± 0.01	0.05 ± 0.02
Cycle 2	$0.00 + 0.00$	$0.00 + 0.00$	$0.00 + 0.01$	0.05 ± 0.01	0.07 ± 0.02
$\Delta R/R_0$ (10^{-3})					
Reversible					
Cycle 1	5.00 ± 0.55	7.80 ± 0.73	12.51 ± 1.11	14.61 ± 1.61	18.40 ± 2.51
Cycle 2	5.00 ± 0.64	7.80 ± 0.92	12.50 ± 1.23	14.58 ± 1.82	18.13 ± 2.84
Irreversible					
Cycle 1	0.00 ± 0.00	0.00 ± 0.00	1.50 ± 0.21	2.20 ± 0.33	4.00 ± 0.78
Cycle 2	0.00 ± 0.00	0.00 ± 0.01	1.52 ± 0.32	2.27 ± 0.54	4.65 ± 0.93
Calculated[a]	3.4	6.3	10.0	11.9	14.1
Gage factor[b]					
Cycle 1	2.27 ± 0.13	1.90 ± 0.76	1.92 ± 0.13	2.00 ± 0.21	2.14 ± 0.19
Cycle 2	2.27 ± 0.14	1.90 ± 0.85	1.92 ± 0.12	2.03 ± 0.22	2.13 ± 0.20
Elastic modulus (GPa)					
1st cycle	230	226	228	221	225
2nd cycle	229	225	225	214	213
Fractional decrease in modulus from 1st to 2nd cycle	0	0	1%	3%	5%

[a]Calculated from change in dimensions.

$$\frac{\Delta R}{R_0} = \frac{1+\varepsilon}{1-2\nu\varepsilon} - 1,$$

where ε = strain and ν = Poisson ratio = 0.27.
[b]Reversible $\Delta R/R_0$ divided by the reversible strain.
[c]5 samples tested.
[d]4 samples tested.
[e]3 samples tested.

TABLE III Carbon fiber and epoxy matrix properties (according to ICI Fiberite)

10E - Torayca T-300 (6 K) untwisted, UC-309 sized	
Diameter	7 μm
Density	1.76 g cm^{-3}
Electrical resistivity	2.2×10^{-3} $\Omega \cdot$ cm
Tensile modulus	221 GPa
Tensile strength	3.1 GPa
976 epoxy	
Process temperature	350 °F (177 °C)
Maximum service temperature	350 °F (177 °C) dry 250 °F (121 °C) wet
Flexural modulus	3.7 GPa
Flexural strength	138 MPa
T_g	232 °C
Density	1.28 g cm^{-3}

Fiberite (Tempe, AZ). The product used was Hy-E 1076E, which consisted of a 976 epoxy matrix and 10E carbon fibers. The fiber and matrix properties are shown in Table III.

The composite laminates were laid up in a 4×7 in. (10×18 cm) platten compression mold with laminate configuration $[0]_8$ (i.e., eight unidirectional fiber layers in the laminate). The individual 4×7 in. (10×18 cm) fiber layers were cut from the prepreg tape. The layers were stacked in the mold with a mold release film on the top and bottom of the layup. No liquid mold release was necessary. The density and thickness of the laminate were 1.52 ± 0.01 g/cm^3 and 1.1 mm respectively. The volume fraction of carbon fibers in the composite was 58%. The laminates were cured using a cycle based on the ICI Fiberite C-5 cure cycle. The curing occurred at 179 ± 6 °C (355 ± 10 °F) and 0.61 MPa (89 psi) for 120 min. Afterward, they were cut to pieces of size 160×14 mm. Hence, each specimen had 38 bundles of fibers (6000 fibers per bundle, 7 μm diameter for each fiber). Glass fiber reinforced epoxy end tabs were applied to both ends on both sides of each piece, such that each tab was 30 mm long and the inner edges of the end tabs on the same side were 100 mm apart and the outer edges were 160 mm apart.

The electrical resistance R was measured in the longitudinal direction using the four-probe method while cyclic tension-tension was applied in the longitudinal direction. Silver paint was used for all electrical contacts. The four probes consisted of two outer current probes and two inner voltage probes. The resistance R refers to the sample resistance between the inner

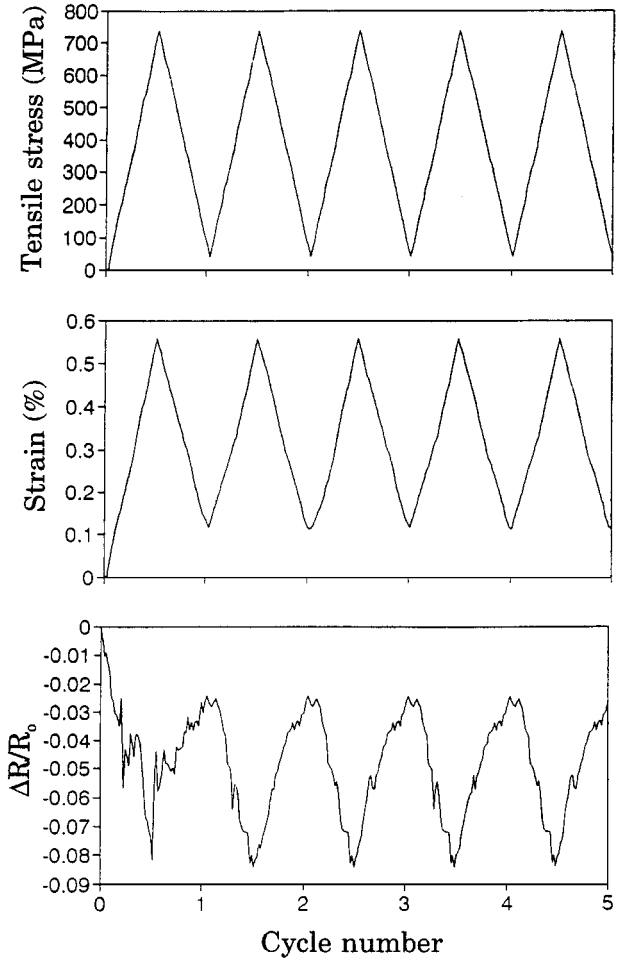

Figure 4 Variation of fractional resistance increase ($\Delta R/R_0$), tensile stress and tensile strain with cycle number during the first few cycles of tension-tension fatigue testing for a carbon fiber polymer-matrix composite.

probes. The four electrical contacts were around the whole perimeter of the sample in four parallel planes that were perpendicular to the stress axis, such that the inner probes were 60 mm apart and the outer probes were 78 mm apart. A strain gage was attached to the center of one of the largest opposite faces. A Keithley 2001 multimeter was used for DC resistance measurement. The displacement rate was 1.0 mm/min. A hydraulic mechanical testing system (MTS 810) was used for tension-tension cyclic loading in the longitudinal direction, with stress ratio (minimum stress to maximum stress in a cycle) 0.05 and maximum stress 740 MPa (at which strain = 0.56%). The fatigue test was run at a constant amplitude load level (load control). Each cycle took 1 s. A total of 396, 854 cycles took place before fatigue failure. Although the results shown in this paper are for one particular fatigue test, testing of similar samples confirmed that the results presented here are reproducible.

Fig. 4 shows the fractional resistance increase ($\Delta R/R_0$), tensile stress and tensile strain simultaneously obtained in the stress (fiber) direction during cyclic tension-tension loading. The strain did not return to zero at the end of each cycle. The resistance R decreased upon loading and increased upon unloading in every cycle, such that R irreversibly decreased after the

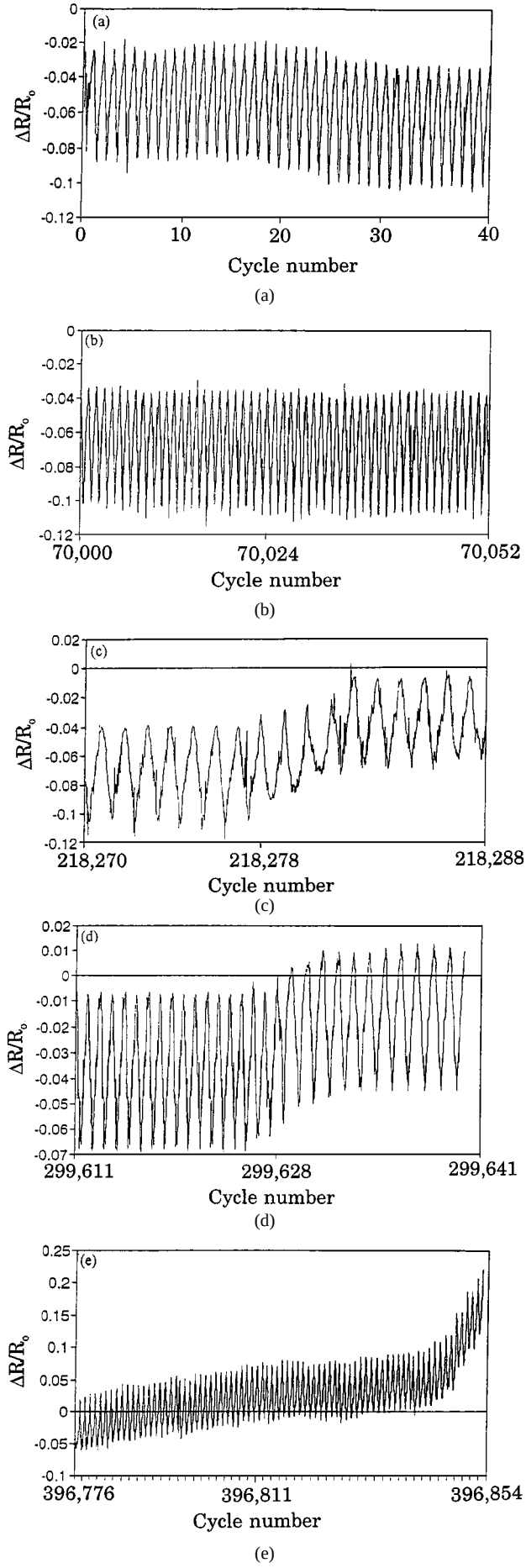

Figure 5 Variation of $\Delta R/R_0$ with cycle number during tension-tension fatigue testing up to failure at 396, 854 cycles for a carbon fiber polymer-matrix composite.

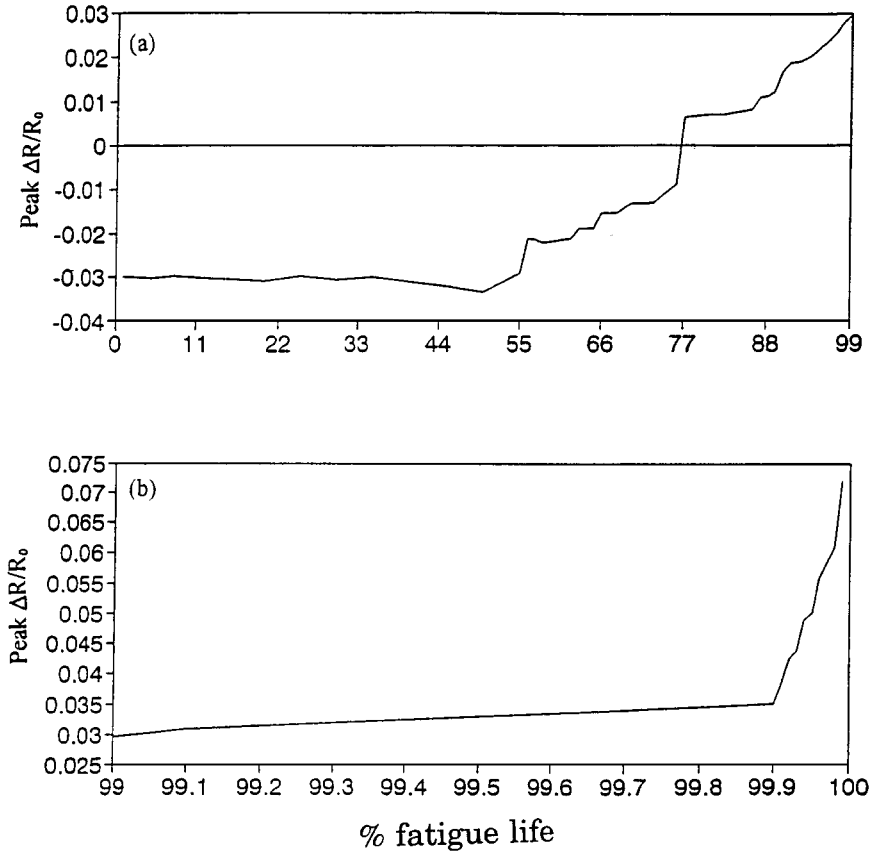

Figure 6 Variation of the peak $\Delta R/R_0$ at the end of a cycle with the percentage of fatigue life during tension-tension fatigue testing up to failure for a carbon fiber polymer-matrix composite.

first cycle, as for the case of the strain being completely reversible. The irreversible decrease in R after the first cycle (even when the strain is completely reversible) is due to the irreversible decrease in the degree of neatness of the fiber arrangement [12]. A length increase without any resistivity change would have caused R to increase during tensile loading. In contrast, R was observed to decrease upon tensile loading. Furthermore, the observed magnitude of $\Delta R/R_0$ was 9–14 times that of $\Delta R/R_0$ calculated by assuming that $\Delta R/R_0$ was only due to length increase and not due to any resistivity change. Hence, the contribution of $\Delta R/R_0$ from the length increase is negligible compared to that from the resistivity change. The reversible decrease in R was attributed to the increase in the degree of fiber alignment (i.e., decrease in the degree of fiber waviness).

As cycling progressed beyond 218, 277 cycles (or 55% of fatigue life), the peak R (at the end of a cycle) significantly but gradually increased, such that the increase did not occur in every cycle, but occurred in spurts (Figs 5 and 6a), e.g., at 218, 278 cycles (Fig. 5c) and 229, 628 cycles (Fig. 5d). Fig. 6 shows the variation of the peak $\Delta R/R_0$ as a function of the percentage of the fatigue life throughout the entire life. Beyond 353, 200 cycles (89% of fatigue life), the increase of the peak R occurred continuously from cycle to cycle rather than in spurts (Fig. 5e). At 396, 457 cycles (99.9% of fatigue life), the increase became more severe, such that spurts of increase occurred on top of the continuous increase (Fig. 6b). The severity kept increasing until failure at 396, 854 cycles, at which R abruptly increased. The last spurt before the final abrupt increase occurred at 396, 842 cycles (99.997% of the fatigue life) (Fig. 5e).

The early period in which the peak R increased discontinuously in spurts is attributed to minor damage in the form of fiber breakage which did not occur in every cycle. The subsequent period in which the peak R increased continuously but gradually is attributed to fiber breakage which occurred in every cycle. The still subsequent period in which the peak R increased rapidly, both in spurts (which did not occur in every cycle) and continuously (i.e., in every cycle), is attributed to more extensive fiber breakage, which occurred in the final period before failure. Thus, by following the increase in the peak R, the degree of damage can be monitored progressively in real time. Moreover, progressive warning of the impending fatigue failure is provided in real time, so disasters due to fatigue failure can be avoided.

The resistance R of a single bare carbon fiber increased upon tension, such that, at a tensile stress equal to 83% of the fracture stress, the reversible portion of $\Delta R/R_0$ (due to dimensional change) was 18.4×10^{-3}, while the irreversible portion of $\Delta R/R_0$ (due to damage) was 4.0×10^{-3} (Section 2). We therefore assumed that a fiber prior to fatigue failure has an irreversible $\Delta R/R_0$ of 4.0×10^{-3}. There are two sources of irreversible $\Delta R/R_0$, namely fiber damage and fiber breakage, though the former was almost negligible compared to the latter. The irreversible $\Delta R/R_0$ due to fiber damage was subtracted from the measured irreversible $\Delta R/R_0$ (in the part of the fatigue life in which the

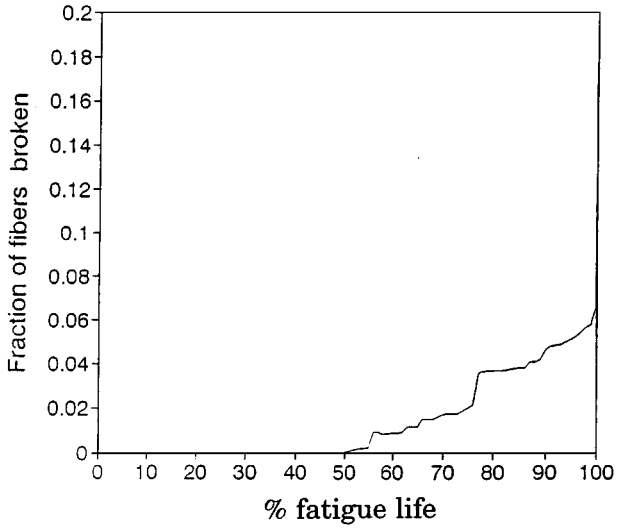

(a)

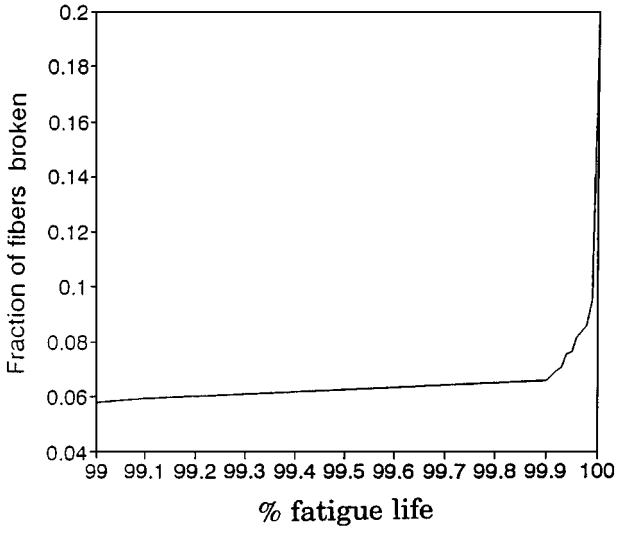

(b)

Figure 7 Variation of the fraction of fibers broken with the percentage of fatigue life during tension-tension fatigue testing up to failure for a carbon fiber polymer-matrix composite. (a) From 0 to 100% of fatigue life. (b) From 99 to 100% of fatigue life.

irreversible $\Delta R/R_0$ had shown an increase from the initial value) in order to obtain the irreversible $\Delta R/R_0$ due to fiber breakage.

Assuming that the resistivity of the undamaged portion of the composite does not change during testing, the fraction of fibers broken is equal to the fractional decrease in the effective cross-sectional area of the unidirectional composite. Hence, in the part of the fatigue life in which the peak R at the end of a cycle had shown an increase from its value R_0' at the end of the first cycle [$R_0' = R_0 + (\Delta R)_0$, where R_0 is the initial resistance and $(\Delta R)_0$ is the ΔR at the end of the first cycle],

$$\text{fraction of fibers broken} = \frac{Q}{1+Q}, \qquad (1)$$

where $Q = (\frac{R-R_0'}{R_0'}) - 4.0 \times 10^{-3}$, R is the peak R at the end of a cycle, and 4.0×10^{-3} is the contribution from fiber damage. Fig. 7 shows a plot of the fraction of fibers broken as a function of the percentage of fatigue life, as obtained by using Equation 1. Fiber breakage started to occur at 50% of the fatigue life, though appreciable growth of the fraction of fibers broken did not start till 55% of the fatigue life. Fiber breakage occurred in spurts from 55 to 89% of the fatigue life, due to fiber breakage not occurring in every cycle. The smallest spurt involved 0.6% of the fibers breaking. This corresponds to 1020 fibers breaking. Thus, each spurt involved the breaking of multiple fibers. This is reasonable since the fibers were in bundles of 6000 fibers. The smallest spurt involved the breaking of a fraction of a fiber bundle. At 89% of the fatigue life, fiber breakage started to occur continuously rather than in spurts. Catastrophic failure occurred when 18% of the fibers were broken.

Damage in the form of delamination can be sensed by measuring the electrical resistance in the through-thickness direction rather than that in the fiber direction. It is the subject of a separate publication [18].

In summary, real-time monitoring of fatigue damage and dynamic strain in a continuous unidirectional carbon fiber polymer-matrix composite by longitudinal electrical resistance measurement was demonstrated. The resistance R decreased reversibly upon tensile loading in every cycle, thus providing dynamic strain monitoring. The peak R in a cycle irreversibly increased as fatigue damage occurred, due mainly to breakage of the carbon fibers. The degree of damage was indicated by the extent of increase of the peak R at the end of a cycle. Fiber breakage started at 50% of the fatigue life, but significant growth of the fraction of fibers broken did not start till 55% of the fatigue life. From 55 to 89% of the fatigue life, fiber breakage occurred in spurts (i.e., not continuously from cycle to cycle), such that each spurt involved the breaking of at least 1000 fibers. At 89% of the fatigue life, damage started to occur continuously from cycle to cycle, but gradually. At 99.9% of the fatigue life, damage started to occur increasingly rapidly, both continuously and in spurts, and this persisted until failure. The last spurt occurred at 99.99% of the fatigue life. Catastrophic failure occurred when 18% of the fibers were broken. Hence, a progressive indication of the amount of remaining fatigue life was obtained in real time.

4. A carbon-matrix composite with continuous carbon fibers

The carbon matrix, though much more high-temperature resistant than a polymer matrix, is much more brittle than a polymer matrix. This brittleness makes carbon-carbon composites prone to matrix cracking. As shown in this section, exceptional sensitivity to even slight damage can be obtained by using the carbon-carbon composite itself as the damage sensor to monitor the composite's own damage. The high sensitivity to damage is due to the high conductivity of the carbon matrix, compared to the polymer matrix (Section 3), and the importance of matrix cracking in the mechanism for damage in a carbon-carbon composite.

Fig. 8 shows the stress (curve (a)) and the fractional DC resistance increase ($\Delta R/R_0$) (curve (b)) obtained

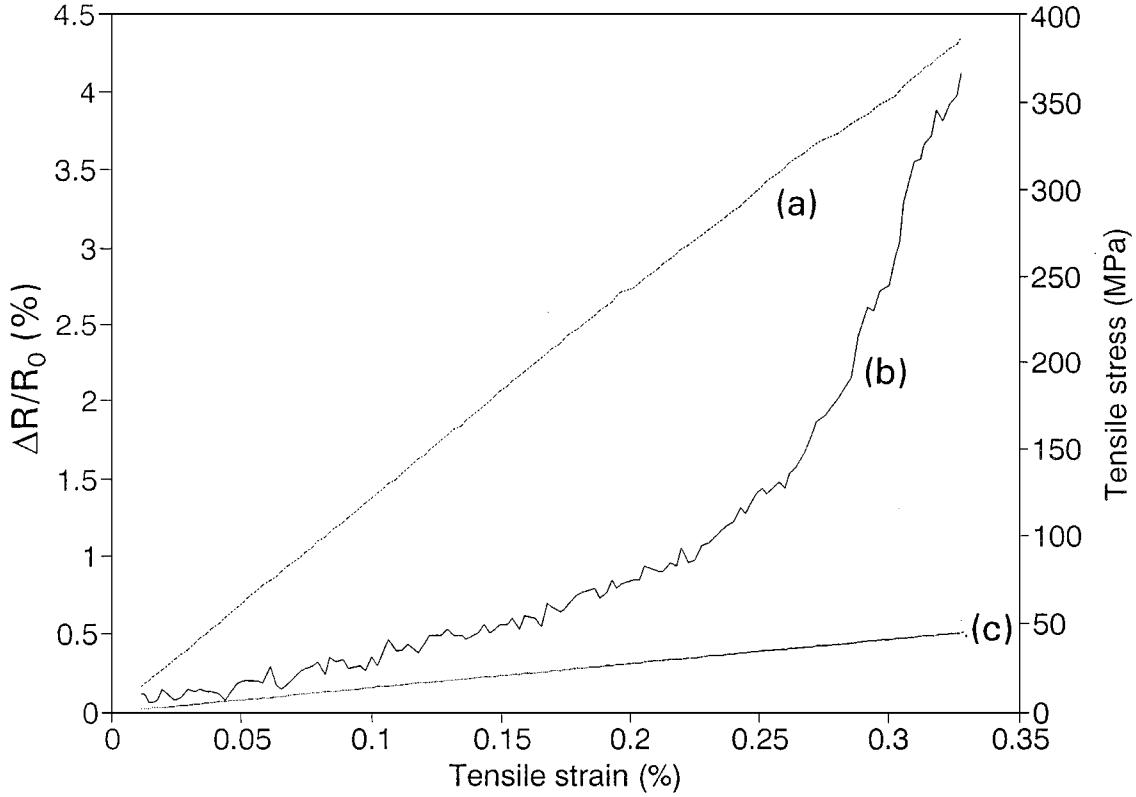

Figure 8 Plots of (a) tensile stress vs. strain, and (b) $\Delta R/R_0$ vs. strain, obtained simultaneously during static tension up to failure for a carbon-carbon composite. Curve (c) is the calculated $\Delta R/R_0$ based on dimensional changes.

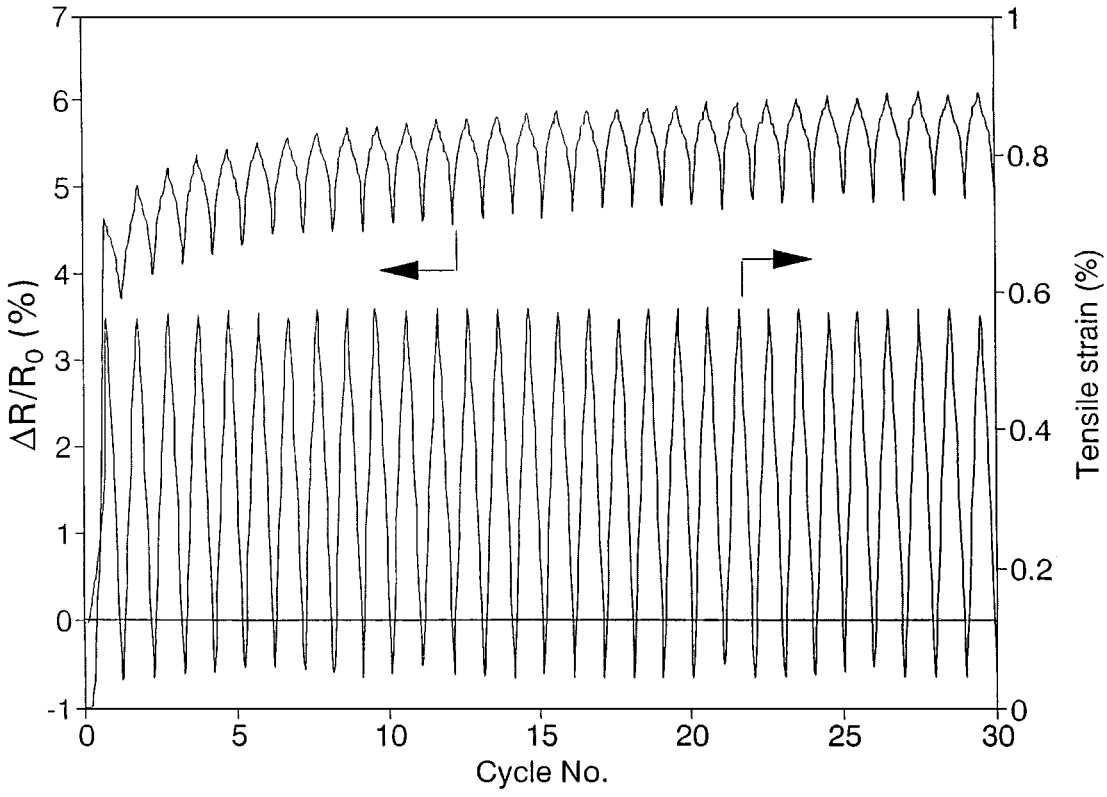

Figure 9 Plots of $\Delta R/R_0$ vs. cycle no. and of tensile strain vs. cycle no., obtained simultaneously during first cyclic tension at a stress amplitude of 94% of the fracture stress for a carbon-carbon composite.

during static tension up to failure for a carbon-carbon composite (provided by Sigri Great Lakes Carbon Corp., Union, NJ) having two-dimensionally (90°) woven fibers and a heat treatment temperature of 2000 °C, with the resistance and stress in the direction of one of the two perpendicular sets of fibers. $\Delta R/R_0$ increased monotonically with strain, such that the increase was gradual (only slightly above the increase in $\Delta R/R_0$ due

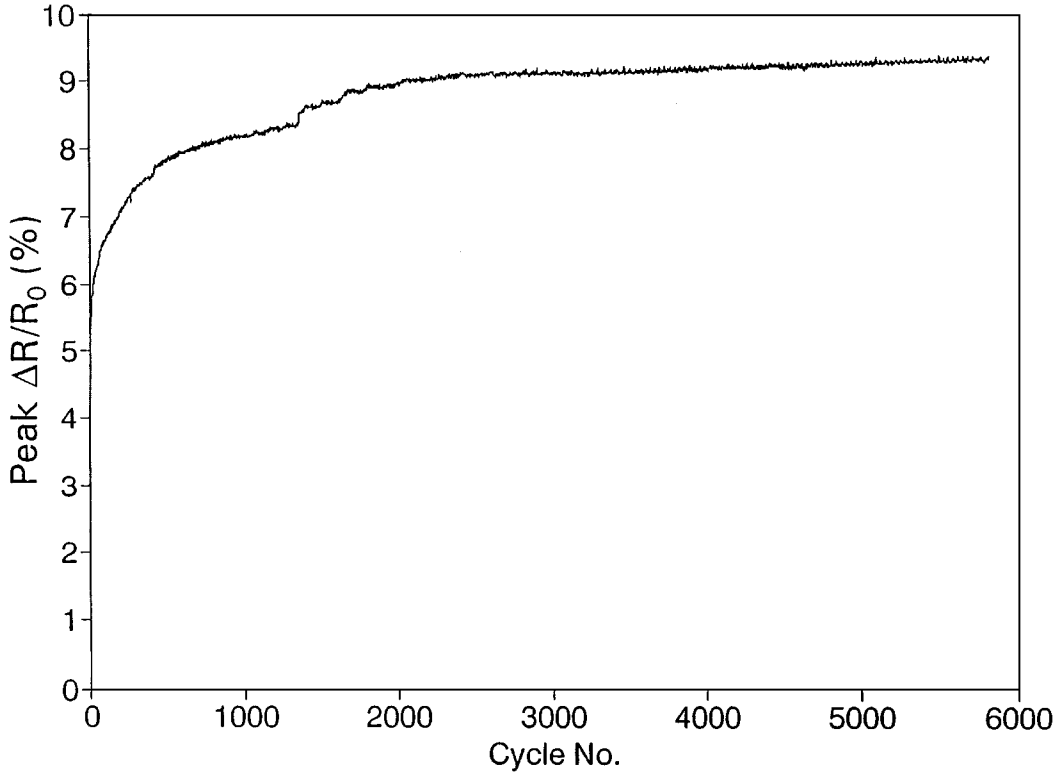

Figure 10 Variation of the peak $\Delta R/R_0$ with cycle no. throughout the entire fatigue life at a stress amplitude of 94% of the fracture stress for a carbon-carbon composite.

to the changes in dimensions, curve (c) in Fig. 8) at low strains and abrupt at high strains.

Fig. 9 shows $\Delta R/R_0$ obtained during cyclic tension to a stress amplitude (360 MPa) equal to 94% of the breaking stress. The tensile strain was almost totally reversible. The irreversible strain was 0.040% at the end of the first cycle, and increased very slightly with increasing cycle number. $\Delta R/R_0$ increased upon loading in every cycle, such that it irreversibly increased slightly after every cycle and the irreversible increase in $\Delta R/R_0$ was particularly large for the first cycle, as shown in Fig. 9. At fatigue failure, $\Delta R/R_0$ abruptly increased, such that $\Delta R/R_0$ did not more rapidly increase irreversibly near the end of fatigue life. Fig. 10 shows the peak $\Delta R/R_0$ values in a cycle as a function of cycle number throughout the fatigue life up to failure. The peak $\Delta R/R_0$ increased with cycle number significantly during the first 500 cycles and gradually during all subsequent cycles up to failure. The small step increases in the peak $\Delta R/R_0$, for example at $\sim$1350 cycles, are not experimental artifacts but are attributed to damage occurring at those cycle numbers, similar to the step increases observed for a continuous carbon fiber polymer-matrix composite under similar cyclic loading (Fig. 6).

The reversible part of $\Delta R/R_0$ is mainly due to reversible dimensional changes and correlates with reversible strain. The irreversible part of $\Delta R/R_0$ is due to damage. Although the increases in irreversible strain and decrease in Young's modulus also indicate damage, the changes in these parameters are very small compared to the change in the irreversible part of $\Delta R/R_0$. The great sensitivity of the irreversible part of $\Delta R/R_0$ to damage is also shown by the significant non-zero value of the irreversible part of $\Delta R/R_0$ after merely the first cycle, even at a stress amplitude of just 20% of the fracture stress (Fig. 11). However, the incremental rise in irreversible $\Delta R/R_0$ beyond $\sim$500 cycles was small. The composite damage probably involved fiber-matrix interface weakening, matrix cracking and fiber breakage; these origins of damage could not be distinguished through the experimental technique used. Nevertheless, the increase of the irreversible part of $\Delta R/R_0$ as cycling progressed provided a continuous indication of the extent of damage. That the reversible part of $\Delta R/R_0$ also increased with cycling and that an abrupt increase of the irreversible part of $\Delta R/R_0$ is associated with an abrupt increase in the reversible part of $\Delta R/R_0$ suggest that the reversible part of $\Delta R/R_0$ is partly associated with a phenomenon which intensifies as damage increases, although it is mostly associated with dimensional changes. This phenomenon may be reversible crack opening during tension, as cracks are expected to increase in size and/or density as cycling progresses. This interpretation is consistent with the observation that an abrupt increase in the reversible part of $\Delta R/R_0$ is associated with an abrupt increase in reversible strain and that the abrupt increase in reversible strain occurs at stress amplitudes beyond the range in which the reversible strain is linear in relation to the stress amplitude.

In summary, the carbon-matrix composite was highly effective for damage sensing (i.e., sensitivity even to the damage after the first cycle of tensile loading within the elastic regime), because the matrix was conducting and its fracture caused the resistivity to increase irreversibly. The carbon-carbon composite was also a strain sensor, due to the dimensional changes during tension and the resulting reversible increase in the resistance.

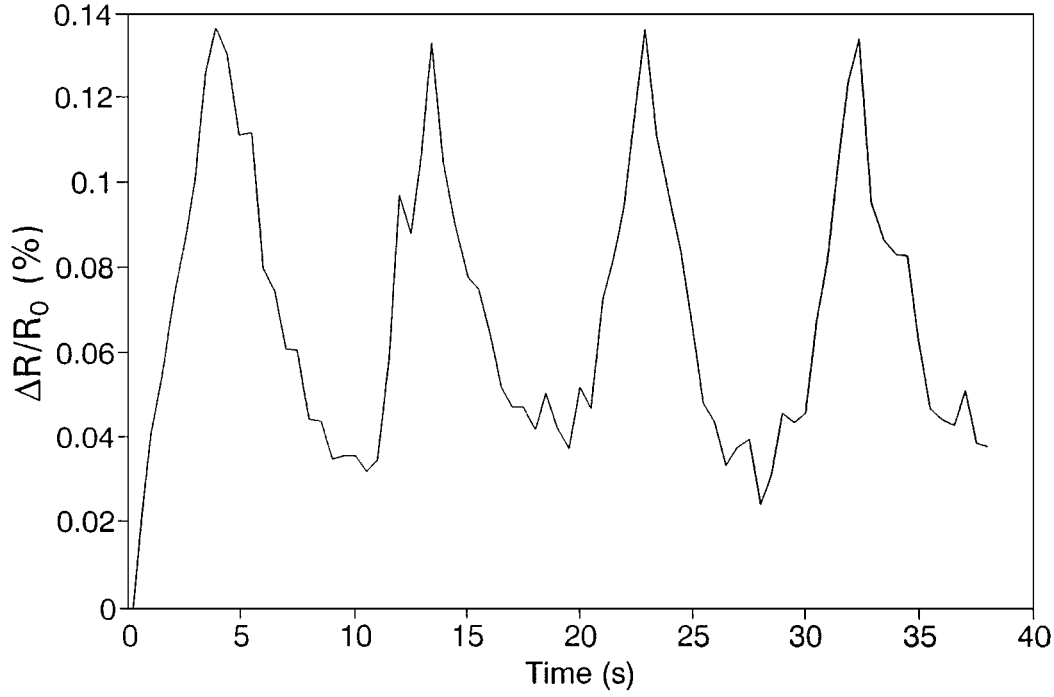

Figure 11 Plot of $\Delta R/R_0$ vs. time during the first four cycles at a stress amplitude of 20% of the fracture stress for a carbon-carbon composite.

5. Conclusion

Fatigue damage in continuous carbon fiber and its polymer-matrix and carbon-matrix composites can be sensed in real time by electrical resistance measurement in the fiber direction. Fiber damage, fiber breakage and, in the case of the carbon-matrix composite, matrix cracking all cause the resistivity of the composite to increase irreversibly. In a polymer-matrix composite, fiber breakage overshadows fiber damage in affecting the resistivity of the composite. From the resistivity increase, the fraction of fibers broken can be obtained. In a carbon-matrix composite, both fiber breakage and matrix cracking contribute significantly to causing the resistivity of the composite to increase irreversibly, such that these two damage mechanisms cannot be distinguished electrically. Due to the sensitivity to matrix cracking and the brittleness of the carbon matrix, damage sensing was exceptionally effective for the carbon-matrix composite. For the polymer-matrix composite, damage was detected from 50% of the fatigue life onward; for the carbon-matrix composite, damage was sensed from 0% of the fatigue life onward.

Acknowledgement

This work was supported in part by Center for Electronic and Electro-Optic Materials, State University of New York at Buffalo.

References

1. C. FISCHER and F. J. ARENTS, *Composites Sci. Tech.* **46** (1993) 319–323.
2. R. PRABHAKARAN, *Experimental Techniques* **14** (1990)16–20.
3. N. MUTO and H. MIYAYAMA, *J. Ceram. Soc. Jpn.* **18** (1992) 144–150.
4. N. MUTO, H. YANAGIDA, M. MIYAYAMA, T. NAKATSUJI, M. SUGITA and Y. OHTSUKA, *ibid.* **100**(4) (1992) 585–588.
5. N. MUTO and H. MIYAYAMA, *Adv. Composite Mater.* **4**(1995) 297–308.
6. M. SUGITA, H. YANAGIDA and N. MUTO, *Smart Mater. Struct.* **4**(1A) (1995) A52–A57.
7. A. S. KADDOUR, F. A. R. AL-SALEHI, S. T. S. AL-HASSANI and M. J. HINTON, *Compos. Sci. Tech.* **51**(3) (1994) 377–385.
8. K. SCHULTE, *J. Physique IV, Colloque* **C7** (1993) 1629.
9. K. SCHULTE and CH. BARON, *Compos. Sci. Tech.* **36** (1989) 63.
10. O. CEYSSON, M. SALVIA and L. VINCENT, *Scripta Materialia* **34** (1996) 1273.
11. N. MUTO, H. YANAGIDA, M. MIYAYAMA, T. NAKATSUJI, M. SUGITA and Y. OHTSUKA, *J. Ceram Soc. Jpn* **100**(4) (1992) 585–588.
12. X. WANG and D.D.L. CHUNG, *Smart Mater. Struct.* **5** (1996) 796–800.
13. P. C. CONOR and C. N. OWSTON, *Nature* **223** (1969) 1146–1147.
14. C. N. OWSTON, *J. Phys.* **D3** (1970) 1615–1626.
15. C. A. BERG, H. CUMPSTON and A. RINSKY, *Textile Research Journal* **42**(8) (1972) 486.
16. S. J. DETERESA, *Carbon* **29**(3) (1991) 397.
17. A. S. CRASTO and R. Y. KIM, Proc. Amer. Soc. Composites, 8th Tech. Conf. (Technomic Pub. Co., Lancaster, PA, 1994) pp. 162–173.
18. X. WANG and D. D. L. CHUNG, *Polymer Composites* **18**(6) (1997) 692–700.

Received 9 June 1997
and accepted 22 January 1999